Contents lists available at ScienceDirect

Physics Letters B

www.elsevier.com/locate/physletb

PHYSICS LETTERS B

Mutual boosting of the saturation scales in colliding nuclei

B.Z. Kopeliovich [a,b,∗], H.J. Pirner [b], I.K. Potashnikova [a], Iván Schmidt [a]

[a] *Departamento de Física, Universidad Técnica Federico Santa María, Instituto de Estudios Avanzados en Ciencias e Ingeniería, Centro Científico-Tecnológico de Valparaíso, Casilla 110-V, Valparaíso, Chile*
[b] *Institut für Theoretische Physik der Universität, Philosophenweg 19, 69120 Heidelberg, Germany*

ARTICLE INFO

ABSTRACT

Saturation of small-x gluons in a nucleus, which has the form of transverse momentum broadening of projectile gluons in pA collisions in the nuclear rest frame, leads to a modification of the parton distribution functions in the beam compared with pp collisions. The DGLAP driven gluon distribution turns out to be suppressed at large x, but significantly enhanced at $x \ll 1$. This is a high twist effect. In the case of nucleus–nucleus collisions all participating nucleons on both sides get enriched in gluon density at small x, which leads to a further boosting of the saturation scale. We derive reciprocity equations for the saturation scales corresponding to a collision of two nuclei. The solution of these equations for central collisions of two heavy nuclei demonstrate a significant, up to several times, enhancement of Q_{sA}^2, in AA compared with pA collisions.

© 2011 Elsevier B.V. Open access under CC BY license.

1. Introduction

The transverse momentum distribution of gluons in nuclei is known to be modified compared with a free nucleon. The mean transverse momentum squared increases up to a value called saturated scale, Q_{sA}^2, which depends on the nuclear profile. This phenomenon, called color glass condensate [1], is related to parton saturation at small x [2], and can be also understood in terms of the Landau–Pomeranchuk principle [3] as a consequence of coherent gluon radiation from multiple interactions in the nucleus [4]. The value of the saturation momentum was calculated and compared with data on broadening in [4] and has been modeled recently in [5–12].

The saturation scale can be measured as p_T-broadening of a parton propagating through the nucleus in its rest frame [4],

$$Q_{sA}^2 = \Delta p_T^2. \tag{1}$$

Although in leading order both sides of this relation rise linearly with nuclear profile T_A [13–17], this dependence slows down by gluon shadowing. These phenomena, broadening and suppression of gluons, are closely related, since both result from coherence of gluon radiation in multiple interactions. Solving the corresponding

equation derived in [4], one arrives at a saturation scale considerably reduced compared to the leading order. The T_A dependence is slower than linear, and at very large (unrealistic) nuclear thicknesses the saturation scale saturates, becoming independent of T_A. Notice that the solution found in [4] is similar to the result of numerical solution [22] of the Balitsky–Kovchegov equation [18,19]. Broadening of gluons radiated in heavy ion collisions was studied with numerical simulations in [20,21].

2. Modification of the beam PDF by a nuclear target

Due to broadening a nuclear target probes the parton distribution in the beam hadron with a higher resolution. Therefore, the effective scale Q^2 for the beam PDF drifts to a higher value $Q^2 + Q_{sA}^2$. At first glance this seems to contradict causality, indeed, how can the primordial parton distribution in the hadron depend on the interaction which happens later? However, there is nothing wrong. The interaction performs a special selection of Fock states in the incoming hadron. The same phenomenon happens when one is measuring the proton parton distribution in DIS. The proton PDF "knows" in advance about the virtuality of the photon which it is going to interact with.

The shift in the scale also can be interpreted as a manifestation of the Landau–Pomeranchuk principle [3]: at long coherence times gluon radiation (which causes the DGLAP evolution) does not depend on the details of multiple interactions, but correlates only with the total momentum transfer, $\vec{q} + \Delta \vec{p}_T$, which after squaring and averaging over angles results in $Q^2 + \Delta p_T^2$.

* Corresponding author at: Departamento de Física, Universidad Técnica Federico Santa María, Instituto de Estudios Avanzados en Ciencias e Ingeniería, Centro Científico-Tecnológico de Valparaíso, Casilla 110-V, Valparaíso, Chile.
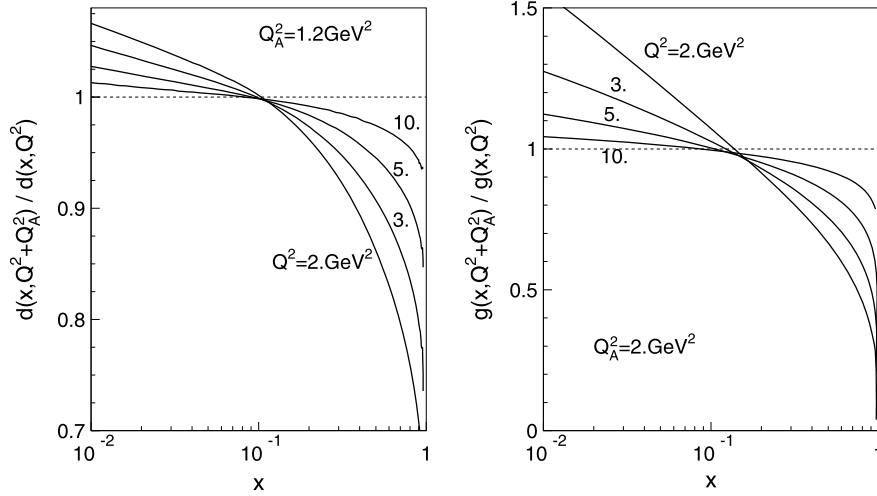*E-mail address:* bzk@mpi-hd.mpg.de (B.Z. Kopeliovich).

Fig. 1. Ratio of parton distribution functions in a reaction characterized by a hard scale $Q^2 = 2, 3, 5, 10$ GeV^2 on a nuclear ($A = 200$) and proton targets. *Left panel*: ratio of the d-quark distributions for the quark saturation momentum $Q_{sA}^2 = 1.2$ GeV^2. *Right panel*: ratio for gluons with the gluon saturation momentum $Q_{sA}^2 = 2$ GeV^2.

As far as the PDF of the projectile proton has a harder scale in pA collisions than in pp, the ratio of parton distributions should fall below one at forward and rise above one at backward rapidities. This may look like a breakdown of k_T-factorization, however, it is a higher twist effect.

Examples of pA to pp ratios $R_A(x, Q^2)$ calculated with MSTW2008 [23] are shown in Fig. 1 for d-quark and gluon distributions in a hard reaction (high-p_T, heavy flavor production, etc.). We see that the shift in the hard scale caused by saturation in the nucleus leads to a sizable suppression in the projectile parton distribution at large $x \to 1$ and enhancement at small $x \ll 1$. We also observe that the magnitude of nuclear modification quickly decreases with Q^2 confirming that this is a high twist effect.

Important for what follows is the observation of a considerably increased population of small-x partons in the projectile proton in pA compared with pp collisions.

3. Nucleus–nucleus collisions: reciprocity relations

Notice that in pA collisions the modification of the PDFs of the beam and target are not symmetric. Namely, the scale of the PDF of the beam proton gets a shift, $Q^2 \Rightarrow Q_{eff}^2 = Q^2 + Q_{sA}^2$, while the PDFs of the bound nucleons, which do not undergo multiple interactions, remain the same as in pp collisions.

The situation changes in the case of a nucleus–nucleus collision: the bound nucleons in both nuclei participate in multiple interactions, therefore the scales of PDFs of all of them are modified. However, this modification goes beyond the simple shift $Q^2 \Rightarrow Q^2 + Q_{sA}^2$. Indeed, in an AB nuclear collision not only the two nucleons (one from A and one from B) participating in the hard reaction undergo multiple interactions, but also many other nucleons, the so-called participants, experience multiple soft interactions. For this reason their parton distributions are boosted from the soft scale μ^2 up to the saturation scale $\mu^2 \Rightarrow \mu^2 + Q_{sA(B)}^2$, which is usually much larger. Thus, the participant nucleons on both sides are boosted to a higher scale and get softer PDFs, with larger parton multiplicities at small x. This is illustrated on the cartoon in Fig. 2.

The next important observation is that the p_T-broadening on such "excited", or boosted nucleons, $\tilde{N}$ is larger than in pA collisions, $\Delta p_T^2|_{\tilde{N}} > \Delta p_T^2|_N$, since the density of target gluons is increased at small x. This should lead to a further mutual enhancement of broadening, i.e. a further increase of the saturation scales
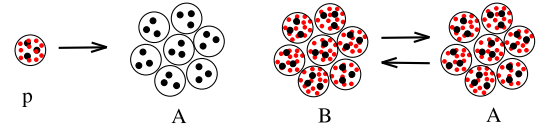

Fig. 2. *Left*: pA collision in which the colliding proton is excited by multiple interactions up to a saturated scale Q_{sA}^2, what leads to an increased multiplicity of soft gluons in the incoming proton. *Right*: nuclear collision in which participating nucleons on both sides are boosted to the saturation scales, Q_{sA}^2 in the nucleus B, and Q_{sB}^2 in the nucleus A. As a result, the low-x gluon population is enriched in both nuclei.

in both nuclei. Intuitively this seems to be clear, but a formal consideration below also supports this conclusion.

Broadening is predominantly a process based on many soft rescatterings of the projectile parton. It was found in [15,14] (see also [4]) that quark broadening is related to the dipole cross section,

$$Q_{sA}^2 = \Delta p_T^2(E) = 2 \frac{d\sigma(r, E)}{dr^2}\bigg|_{r=0} \int dz\, \rho_A(b, z), \qquad (2)$$

where $\rho_A(b, z)$ is the nuclear density at impact parameter b and longitudinal coordinate z. Since the process is soft, Bjorken x is not a proper variable, but instead the parton energy E should be used. The energy dependent $\bar{q}q$ dipole cross section was parametrized in the saturated form and fitted to photoabsorption, low Q^2 DIS data, and πp total cross section in [28] (see also [15,24]). With that parametrization [15]

$$C_q(E) \equiv \frac{d\sigma(r, E)}{dr^2}\bigg|_{r=0} = \frac{1}{4}\sigma_{tot}^{\pi p}(E)\left[Q_{qN}^2(E) + \frac{3}{2\langle r_{ch}^2\rangle_\pi}\right], \qquad (3)$$

where $\sigma_{tot}^{\pi p}(E)$ is the πp total cross section; $\langle r_{ch}^2\rangle_\pi \approx 0.44$ fm^2 is the mean pion charge radius squared; $Q_{qN}(E) = 0.19$ GeV $\times$ $(E/1$ GeV$)^{0.14}$ is the proton saturation momentum.

Notice, that Eq. (3) $C_q(E)$ has no scale dependence. It corresponds to the dipole–nucleon cross section $\sigma_{dip}(r) = C_q r^2$ and a soft scale characterizing the proton is implicitly contained in C_q. Strictly speaking, however, this coefficient is divergent at $r \to 0$, since it contains $\ln(r_T)$ [27]. This divergency originates from the ultraviolet behavior of the unintegrated gluon density $\mathcal{F}(x, k_T) \propto 1/k_T^4$ at large k_T. In reality this divergency is not harmful due to the natural cut-offs discussed in [15], and to a low sensitivity to their values. One should fix the $\ln r$ dependent factor term in C_q at
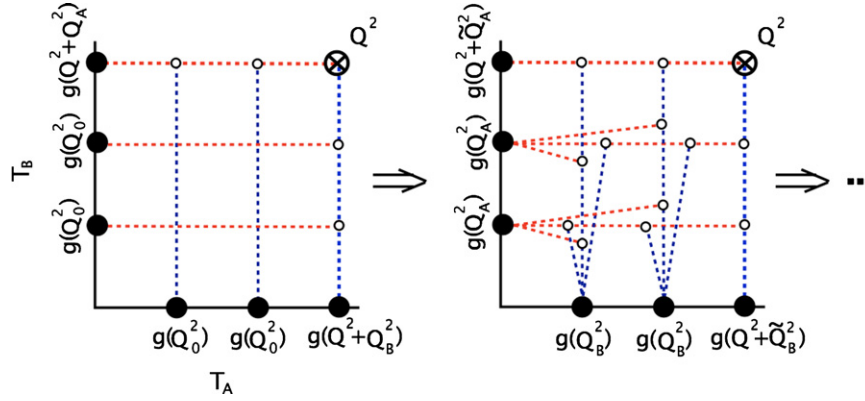
Fig. 3. Collision of two one-dimensional rows of nucleons T_A and T_B displayed on horizontal and vertical axes. Multiple interactions of colliding gluons propagated through both nuclei, including additional multiple scatterings of gluons, which carry out the interactions, are shown as is described in text.

some value of r typical for the process under consideration, as is done in Eq. (3).

The function $C_q(E)$ in (3) describes broadening in pA collisions, resulting from multiple interactions with "normal" target nucleons, whose parton distributions are the same as in pp interactions. However, as was discussed above, the wave functions of participant nucleons in AA collisions are biased towards a larger scale Q_s^2 and a higher multiplicity of the constituent partons. This is why the C_q in (3) acquires the second variable, a scale $Q^2 = Q_s^2$, $C_q(E) \Rightarrow C_q(E, Q^2)$. To expose this scale dependence explicitly, we present the function $C_q(E, Q^2)$ in the form [25,26],

$$C_q(E, Q^2) = \frac{\pi^2}{3}\alpha_s(Q^2)xg_N(x, Q^2), \tag{4}$$

where $g_N(x, Q^2)$ is the gluon distribution function in the target nucleon, and $x = Q^2/2m_N E$.

One should be careful bridging Eq. (4) with its soft limit Eq. (3), since $\alpha_s(Q^2)$ and $g_N(x, Q^2)$ are ill defined at small Q^2. To regularize this problem we replace $Q^2 \Rightarrow Q^2 + Q_0^2$, where Q_0^2 should be adjusted to the reproduction of the correct infra-red limit,

$$\frac{\pi^2}{3}\alpha_s(Q_0^2)xg_N(x, Q_0^2) = C_q(E = Q_0^2/2m_N x). \tag{5}$$

Apparently, the value of Q_0^2 is not universal. It depends on s, x, and most of all on the PDF-analysis dependent behavior of $g_N(x, Q_0^2)$, especially at small Q^2. Here we follow this procedure.

Thus, a participating nucleon simultaneously plays the roles of a beam and of a target. As a beam hadron its PDF is boosted to a higher scale due to multiple interactions it undergoes in another nuclei. As a target such a nucleon, being boosted to a higher scale $Q_0^2 \Rightarrow Q_0^2 + Q_{sB}^2$, it increases broadening of partons from another nucleus, since the factor $C_q(E, Q^2)$ Eq. (4) rises. This leads to a mutual enhancement of the saturation scales in both nuclei. Indeed, multiple rescatterings of nucleons from the nucleus A on the boosted nucleons in B proceed with a larger cross section, so broadening, i.e. the saturation scale in B increases, $Q_{sB}^2 \Rightarrow \tilde{Q}_{sB}^2 > Q_{sB}^2$. For this reason, the nucleon PDFs in A get boosted more. Then the partons from B experience even stronger multiple interactions with such double-boosted nucleons in A. This results in an additional boost of the saturation scale in A, then, as a result, in B, and so on.

Such a multi-iteration mutual boosting of the saturation scales is illustrated pictorially in Fig. 3, where two raws of nucleons, T_A and T_B are displayed on horizontal and vertical axes. In the left picture a gluon originated from one of the nucleons in A (the rightmost vertical dashed line) propagates through B interacting

multiply via gluon exchanges (horizontal dashed lines) and increasing its transverse momentum squared by $\Delta p_T^2 = Q_{sB}^2$. In a similar way a gluon from B (the upper red line) interacts multiply propagating through A and gets broadening Q_{sA}^2. All multiple interactions occur at the soft scale Q_0^2. The two gluons collide (the cross in the upper right corner) at hard scale Q^2, but the original gluon distributions in the colliding nucleons are shifted to higher scales, $Q^2 + Q_{sA}^2$ and $Q^2 + Q_{sB}^2$ respectively.

Then we observe that the t-channel gluon exchanges (vertical lines) between the gluon originated from B and nucleons bound in A, become s-channel gluons propagating through B, after a Lorentz boost between the rest frames of nuclei A and B. Therefore, such gluons should also undergo multiple collisions with nucleons in B. This is shown by additional horizontal gluon lines in the right picture of Fig. 3. And vice versa, the original gluonic exchanges carrying out multiple interactions in the rest frame of B, propagate through A and also experience new multiple interactions, as is depicted in the right-hand side of Fig. 3. These additional interactions boost each of the multiple interactions to a new scale, as well as the scale of the hard reaction $Q_{sA(B)}^2 \Rightarrow \tilde{Q}_{sA(B)}^2$.

In the next iteration (not shown in Fig. 3) the new exchanged gluons also experience multiple scatterings, and so on. The final gluon saturation scales $\tilde{Q}_s^2$ in the collision of two rows of nucleons T_A and T_B can be found solving the reciprocity equations ($C_q \Rightarrow C_g = \frac{9}{4}C_q$),

$$\tilde{Q}_{sB}^2(x_B) = \frac{3\pi^2}{2}\alpha_s(\tilde{Q}_{sA}^2 + Q_0^2)x_B g_N(x_B, \tilde{Q}_{sA}^2 + Q_0^2)T_B;$$

$$\tilde{Q}_{sA}^2(x_A) = \frac{3\pi^2}{2}\alpha_s(\tilde{Q}_{sB}^2 + Q_0^2)x_A g_N(x_A, \tilde{Q}_{sB}^2 + Q_0^2)T_A. \tag{6}$$

These equations are the main result of the paper. Compared to Eq. (3) these equations take into account the modification of the properties of bound nucleons in each of the colliding nuclei due to multiple interactions in another nucleus and the following increase of the scale. Notice that the values of Q_0 in the first and the second equations (6) depend on x_A and x_B respectively, and therefore might be slightly different, but we use the same symbols to simplify the notations.

The reciprocity equations should be solved numerically, but here we estimate the magnitude of the effect for the case of central collision of identical nuclei, i.e. $T_A = T_B$, and a glue–glue collision at mid-rapidity, $x_A = x_B = x$. In this case the system of equations (6) reduces to a single one,

$$\tilde{Q}_{sA}^2(x) = \frac{3\pi^2}{2}\alpha_s(\tilde{Q}_{sA}^2 + Q_0^2)xg_N(x, \tilde{Q}_{sA}^2 + Q_0^2)T_A. \tag{7}$$
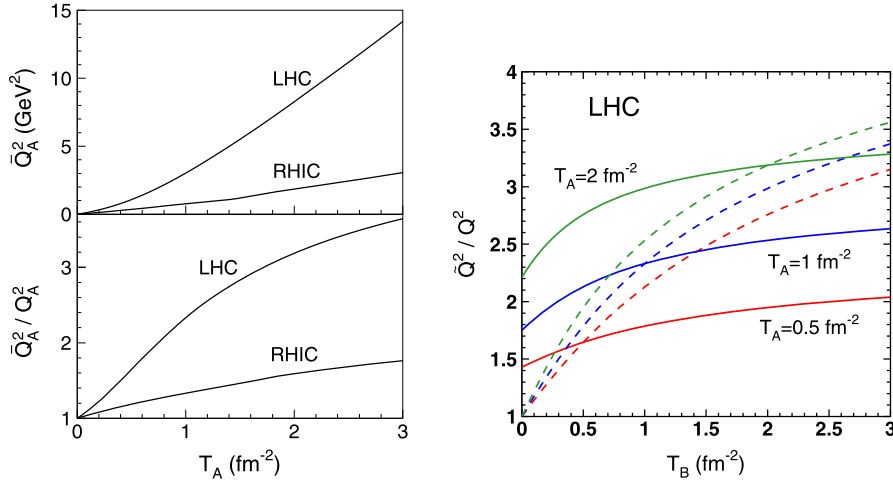
Fig. 4. *Left upper panel*: the boosted values of the saturation momentum squared $\tilde{Q}_{sA}^2$ calculated for $T_A = T_B$ with Eq. (7) at the energies of RHIC and LHC as function of nuclear thickness. *Left bottom panel*: the boosting factors $\tilde{Q}_{sA}^2/Q_{sA}^2$ as function of nuclear thickness. *Right panel*: the boosting factors as function of T_B for fixed values of $T_A = 2, 1, 0.5$ fm^{-2} from bottom to upper curves respectively. Solid and dashed curves correspond to the boosting factors for nuclei B and A respectively.

The scale characterizing multiple interactions of gluons is the mean transverse momentum of gluons $\langle k_T \rangle \approx 0.65$ GeV [28,29]. Therefore, the gluon distribution should be taken at $x = \langle k_T \rangle/\sqrt{s}$, which gives $x = 3.25 \times 10^{-3}$ and $x = 1.18 \times 10^{-4}$, corresponding to $\sqrt{s} = 200$ GeV (RHIC) and 5.5 TeV (LHC) respectively.

To proceed further we should fix the infra-red cutoff Q_0^2 given by Eq. (5). At the energy of RHIC the parameter in the right-hand side of Eq. (5) $C(E = 65 \text{ GeV}) = 3.2$. Then Eq. (5) results in $Q_0^2(\sqrt{s} = 200 \text{ GeV}) = 1.84$ GeV^2. At the energy of LHC the factor $C(E = 1.787 \text{ TeV}) = 7.03$. So we found $Q_0^2(\sqrt{s} = 5.5 \text{ TeV}) = 1.7$ GeV^2. These figures confirm our expectation of a weak energy dependence of the infra-red cutoff Q_0.

With these values of x and Q_0 we solved Eq. (7) for a central collision of identical nuclei, relative to the modified value of the saturation momentum $\tilde{Q}_{sA}$ as function of $T_A = T_B$ using the LO gluon distributions of the recent analysis MSTW2008 [23]. The results are plotted in the left upper panel of Fig. 4 as function of nuclear thickness T_A at the energies of RHIC and LHC. We see that the saturation scale of heavy nuclei may be as large as about 10 GeV^2 at the LHC.

To see the magnitude of the boosting effect we also show in the left bottom panel the boosting factor as function of $T_A = T_B$ at the energies of RHIC and LHC. The enhancement is significant, especially at the energy of LHC, where it reaches a factor of three.

We also solved the reciprocity equations (6) for non-central collisions, i.e. for $T_A \neq T_B$. The boosting factor is plotted in the right panel of Fig. 4 as function of T_B for fixed values of $T_A = 2$, 1, 0.5 fm^{-2} from bottom to upper curves respectively. Solid and dashed curves show the boosting factor for nuclei B and A respectively. These results confirm the expectation illustrated pictorially in the left panel of Fig. 2. Namely, in the limit $T_B \to 0$, corresponding to pA collisions, the boosting effect in nucleus A vanishes, while the parton distribution in the projectile proton is drifting to a higher scale, i.e. the boosting factor exceeds unity. At larger values of T_B the numerical results in Fig. 4 show that the saturation scales in both nuclei are boosted to higher values in accordance with Fig. 2, right.

4. Gluon shadowing

The gluon density at small x in nuclei is expected to be reduced compared with free nucleons. This phenomenon called gluon shadowing, is a part of saturation, but it also affects and diminishes the saturation scale. With this observation we formulated an equation

for the modified saturation scale in pA collisions [4]. The found reduction of the saturation momentum is significant and is similar to the result of numerical solutions [22] of the Balitsky–Kovchegov equation [18,19]. Thus, both Q_{sA}^2 and $\tilde{Q}_{sA}^2$ plotted in the upper panel of Fig. 4 would be reduced in accordance with Ref. [4] (see Fig. 3 of that paper).

However, the modification of the saturation scale due to mutual boosting in heavy ion collisions turns out to be practically unaffected by gluon shadowing. Indeed, either the usual saturation scale Eq. (4), or the reciprocity equations (6) are controlled by the gluon distribution function, which should be modified in a nucleus by a factor $R_g(x, Q^2, T_A)$, which is the nucleus-to-nucleon ratio of the gluon PDFs. The difference between the two is in the scales for gluons shadowing, which are Q_{sA}^2 and $\tilde{Q}_{sA}^2$ respectively. However, the scale dependence of $\alpha_s(Q^2)g(x, Q^2)$ at small x, given by the DGLAP evolution, is very slow and can be neglected. Thus, the boosting factors depicted in the bottom panel of Fig. 4 are not affected by gluon shadowing.

5. Experimental observables

Increase of the saturation scales in colliding nuclei should certainly lead to a rise of transverse momenta of produced hadrons in comparison with an extrapolation from pA collisions. However, final state interactions with the dense medium created in heavy ion collisions, significantly modify the transverse momentum distribution of produced hadrons. Exclusion is production of heavy quarkonia. Propagating through a dense medium they experience no energy loss, and their survival probability is practically independent of p_T. Therefore any observed modifications of the p_T-distribution of heavy quarkonia produced in nuclear collisions should be associated with initial state interactions. This fact makes them an excellent for study of gluon broadening in colliding nuclei.

We expect an increased magnitude of broadening J/Ψ and Υ produced in AA compared with pA collisions for the same path length in nuclear medium. This could be interpreted as a signal of the effect of boosted saturation scale discussed here.

Fig. 5 presents RHIC data [30] at $\sqrt{s} = 200$ GeV for the mean J/Ψ transverse momentum squared versus the mean nuclear thickness covered by the projectile gluon in the rest frame of each of the colliding nuclei, calculated at impact parameter of collisions, $\vec{b}$, corresponding to the measured centrality bin,
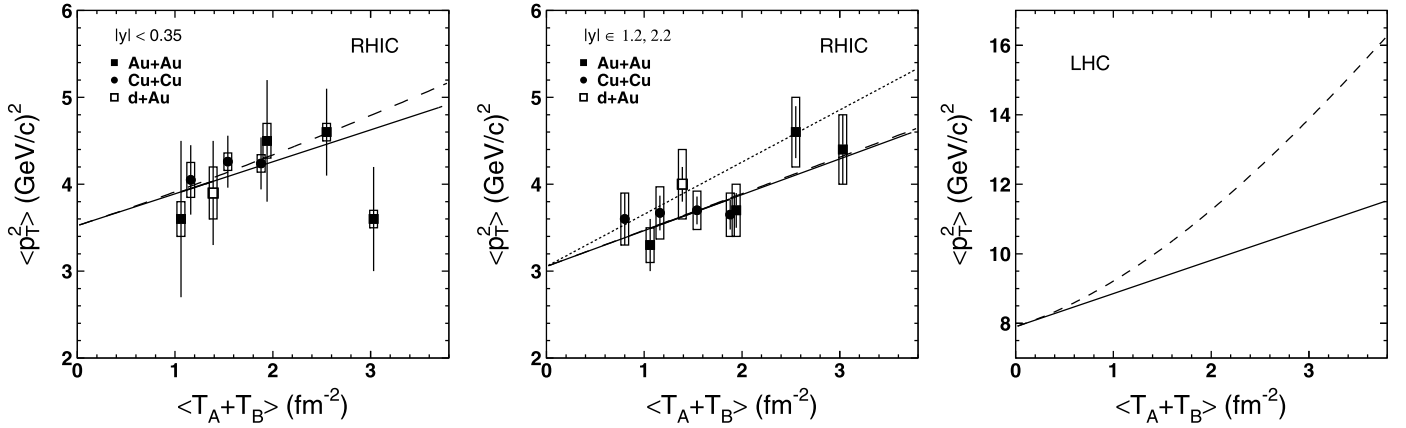
Fig. 5. Data [30] for the mean transverse momentum squared of J/Ψ produced at $\sqrt{s} = 200$ GeV an at $y = 0$ (left panel) and $y = 1.2$–2.2 (middle panel) plotted as function of $\langle T_A + T_B \rangle$ defined in (8). Solid and dashed curves are calculated for AA collision without and with the boosting effect. Same for $\sqrt{s} = 5.5$ TeV is shown in the right panel. The d–Au point in the middle plot should be compared with the dotted curve.

$$\langle T_A + T_B \rangle = \frac{1}{T_{AB}(b)} \int d^2 s \left[T_A(\vec{s}) + T_B(\vec{b} - \vec{s}) \right] T_A(\vec{s}) T_B(\vec{b} - \vec{s}),$$

(8)

where $T_{AB}(b) = \int d^2 s\, T_A(\vec{s}) T_B(\vec{b} - \vec{s})$. Data are compared with the prediction based on Eq. (2) applied to J/Ψ production (see details in [4]) depicted by solid and dotted curves for Au–Au and d–Au collisions respectively. These curves must coincide at $y = 0$ (left panel), but are different at forward rapidities (middle panel), where $x_A \neq x_B$, and we fixed rapidity at $\langle y \rangle = 1.7$. We predict here only broadening, i.e. the slope of the curves, while the absolute value of $\langle p_T^2 \rangle$, which is model dependent and has not been calculated so far, is treated as a fitting parameter.

We also solved Eqs. (6) applied to J/Ψ production, and plotted the result by dashed curves. While at the mid rapidity (left panel) the effect boosting is sizable, although not strong, at forward rapidities (middle panel) it is hardly visible. This is a result of compensation between the effects of rising and decreasing Bjorken x is the two nuclei.

Within the rather large error bars data agree with the theoretical expectations, but cannot resolve the weak boosting effect. Extrapolated to small values of $\langle T_A + T_B \rangle$ all curves should meet at the value of $\langle p_T^2 \rangle$ for pp collisions. We found $\langle p_T^2 \rangle_{pp} = 3.52 \pm 0.3$ GeV^2 and 3.06 ± 0.3 at $y = 0$ and 1.7 respectively, which agree within the errors with the measured values [30].

A much stronger boosting effect for broadening of J/Ψ is expected at LHC. An example at $\sqrt{s} = 5.5$ TeV at $y = 0$ is plotted in the right panel of Fig. 5. Broadening in AA collisions is enhanced up to factor three compared with pA collisions at the same path length in nuclear matter.

Notice, that this kind of enhancement for broadening in AA compared to pA collisions was observed recently in high statistics measurement of J/Ψ production in the NA60 and NA50 experiments at $E_{lab} = 158$ GeV [31]. The magnitude of broadening in nuclear collisions was found twice as big as in pA measurements for the same path length in a nuclear medium. The magnitude of the observed boosting is much larger than follows from Eqs. (6) at this energy, and is probably related to another mechanism enhancing broadening in AA collisions due to interaction with gluons radiated in the preceding multiple collisions [32]. This mechanism correctly predicted the magnitude of the effect observed in the NA50/60 experiments. However, this contribution steeply falls with energy [32], and is negligible at the energies of RHIC and LHC.

Another observable sensitive to the saturation scale is hadron multiplicity [8,33]. In this case the boosting effect should lead to a jump of multiplicity in pA and AA collisions at the same number of participants. Indeed, such a discontinuity was observed [34,35] in data for Au–Au and Cu–Cu collisions at $\sqrt{s} = 200$ GeV in comparison with multiplicity dA and pp collisions. The magnitude of the observed enhancement is in accord with the boosting factors presented in Fig. 4. A detailed analysis of the data and comparison with theoretical expectations goes beyond the scope of this Letter, and will be published separately.

6. Summary

Nuclear targets have a larger resolution than a proton for parton distribution in the projectile hadrons. As a result, the projectile parton distribution is suppressed at large x and enhanced at small x.

The increase of projectile parton densities in the case of nuclear collisions becomes a source of enhancement of the broadening experienced by the target partons propagating through the projectile nucleus, i.e. to an increase of the saturation momentum in the beam (see Fig. 4). Such a mutual enhancement of the saturation scales leads to the system of reciprocal equations (6).

We solved the equations for central heavy ion collision and found the saturation scale for gluon radiation to be boosted up to a factor 1.5 at the energy of RHIC and a factor 3 at LHC.

The saturation scale in nuclear collisions can be probed by measuring broadening of heavy quarkonia, which is not affected by final state interaction with the created dense medium. At the energy of RHIC the boosting effect is too weak to be observed in the currently available data for J/Ψ production, however it should be easily detected at the energies of LHC.

References

[1] L.D. McLerran, R. Venugopalan, Phys. Rev. D 49 (1994) 2233;
     L.D. McLerran, R. Venugopalan, Phys. Rev. D 49 (1994) 3352;
     L.D. McLerran, R. Venugopalan, Phys. Rev. D 50 (1994) 2225.
[2] L.V. Gribov, E.M. Levin, M.G. Ryskin, Nucl. Phys. B 188 (1981) 555;
     L.V. Gribov, E.M. Levin, M.G. Ryskin, Phys. Rep. 100 (1983) 1.

[3] L.D. Landau, I.Ya. Pomeranchuk, Zh. Eksp. Teor. Fiz. 24 (1953) 505;
L.D. Landau, I.Ya. Pomeranchuk, Doklady AN SSSR 92 (1953) 735;
E.L. Feinberg, I.Ya. Pomeranchuk, Doklady AN SSSR 93 (1953) 439;
I.Ya. Pomeranchuk, Doklady AN SSSR 96 (1954) 265;
I.Ya. Pomeranchuk, Doklady AN SSSR 96 (1954) 481;
E.L. Feinberg, I.Ya. Pomeranchuk, Nuovo Cimento Suppl. 4 (1956) 652.
[4] B.Z. Kopeliovich, I.K. Potashnikova, I. Schmidt, Phys. Rev. C 81 (2010) 035204,
arXiv:1001.4281 [hep-ph].
[5] F. Gelis, T. Lappi, R. Venugopalan, Phys. Rev. D 78 (2008) 054019;
F. Gelis, T. Lappi, R. Venugopalan, Phys. Rev. D 78 (2008) 054020;
F. Gelis, T. Lappi, R. Venugopalan, Phys. Rev. D 79 (2009) 094017.
[6] D. Kharzeev, M. Nardi, Phys. Lett. B 507 (2001) 121.
[7] D. Kharzeev, E. Levin, Phys. Lett. B 523 (2001) 79.
[8] D. Kharzeev, E. Levin, M. Nardi, Nucl. Phys. A 730 (2004) 448;
D. Kharzeev, E. Levin, M. Nardi, Nucl. Phys. A 743 (2004) 329, Erratum.
[9] J. Jalilian-Marian, Y.V. Kovchegov, Prog. Part. Nucl. Phys. 56 (2006) 104, arXiv:
hep-ph/0505052.
[10] A. Kuhlman, U.W. Heinz, Y.V. Kovchegov, Phys. Lett. B 638 (2006) 171,
arXiv:nucl-th/0604038.
[11] R. Baier, A. Kovner, U.A. Wiedemann, Phys. Rev. D 68 (2003) 054009, arXiv:
hep-ph/0305265.
[12] A. Kovner, U.A. Wiedemann, Phys. Rev. D 66 (2002) 051502, arXiv:hep-ph/
0112140.
[13] P. Chiappetta, H.J. Pirner, Nucl. Phys. B 291 (1987) 765.
[14] J. Dolejsi, J. Hufner, B.Z. Kopeliovich, Phys. Lett. B 312 (1993) 235, arXiv:
hep-ph/9305238.
[15] M.B. Johnson, B.Z. Kopeliovich, A.V. Tarasov, Phys. Rev. C 63 (2001) 035203.
[16] R. Baier, Y.L. Dokshitzer, A.H. Mueller, S. Peigne, D. Schiff, Nucl. Phys. B 484
(1997) 265, arXiv:hep-ph/9608322.

[17] H. Kowalski, T. Lappi, R. Venugopalan, Phys. Rev. Lett. 100 (2008) 022303,
arXiv:0705.3047 [hep-ph].
[18] I. Balitsky, Nucl. Phys. B 463 (1996) 99.
[19] Y.V. Kovchegov, Phys. Rev. D 60 (1999) 034008.
[20] A. Krasnitz, Y. Nara, R. Venugopalan, Nucl. Phys. A 717 (2003) 268.
[21] T. Lappi, Phys. Rev. C 67 (2003) 054903.
[22] J.L. Albacete, N. Armesto, J.G. Milhano, C.A. Salgado, U.A. Wiedemann, Phys. Rev.
D 71 (2005) 014003, arXiv:hep-ph/0408216.
[23] A.D. Martin, W.J. Stirling, R.S. Thorne, G. Watt, Eur. Phys. J. C 63 (2009) 189;
A.D. Martin, W.J. Stirling, R.S. Thorne, G. Watt, Eur. Phys. J. C 64 (2009) 653.
[24] J. Hufner, Yu.P. Ivanov, B.Z. Kopeliovich, A.V. Tarasov, Phys. Rev. D 62 (2000)
094022, arXiv:hep-ph/0007111.
[25] L. Frankfurt, A. Radyushkin, M. Strikman, Phys. Rev. D 55 (1997) 98.
[26] J. Bartels, K.J. Golec-Biernat, H. Kowalski, Phys. Rev. D 66 (2002) 014001,
arXiv:hep-ph/0203258.
[27] B.Z. Kopeliovich, L.I. Lapidus, A.B. Zamolodchikov, JETP Lett. 33 (1981) 595,
Pisma Zh. Eksp. Teor. Fiz. 33 (1981) 612.
[28] B.Z. Kopeliovich, A. Schäfer, A.V. Tarasov, Phys. Rev. D 62 (2000) 054022.
[29] B.Z. Kopeliovich, I.K. Potashnikova, B. Povh, I. Schmidt, Phys. Rev. D 76 (2007)
094020.
[30] A. Adare, et al., PHENIX Collaboration, Phys. Rev. Lett. 101 (2008) 122301.
[31] P. Cortese, et al., Na60 Collaboration, Talk presented at the 3rd International
Conference on Hard and Electromagnetic Probes of High-Energy Nuclear Colli-
sions, Illa de A Toxa, Galicia, Spain, June 8–14, 2008.
[32] J. Hüfner, B.Z. Kopeliovich, Phys. Lett. B 445 (1998) 223.
[33] D. Kharzeev, E. Levin, M. Nardi, Phys. Rev. C 71 (2005) 054903;
D. Kharzeev, E. Levin, M. Nardi, Nucl. Phys. A 747 (2005) 609.
[34] B. Alver, et al., Phys. Rev. Lett. 102 (2009) 142301.
[35] B. Alver, et al., arXiv:1011.1940 [nucl-ex].